







Article

FLUKA Simulations of $K\beta/K\alpha$ Intensity Ratios of Copper in Ag–Cu Alloys

Aneta Maria Gójska * , Karol Koziol , Adam Wasilewski , Ewelina Agnieszka Miśta-Jakubowska , Piotr Mazerewicz  and Jakub Szymanowski 

National Centre for Nuclear Research, ul. A. Soltana 7, 05-480 Otwock, Poland; karol.koziol@ncbj.gov.pl (K.K.); adam.wasilewski@pwr.edu.pl (A.W.); ewelina.mista@ncbj.gov.pl (E.A.M.-J.); piotr.mazerewicz@ncbj.gov.pl (P.M.); jakub.szymanowski@ncbj.gov.pl (J.S.)

* Correspondence: aneta.gojska@ncbj.gov.pl

Abstract: The numerical simulations of Cu $K\alpha$ and Cu $K\beta$ fluorescence lines induced by Rh X-ray tube and by monoenergetic radiation have been presented. The copper $K\beta/K\alpha$ intensity ratios for pure elements as well as for Ag–Cu alloys have been modeled. The results obtained by use of the FLUKA code, based on the Monte-Carlo approach, have been compared to available experimental and theoretical values. A visible relationship was found between the simulated $K\beta/K\alpha$ intensity ratios and the copper content of the Ag–Cu alloy: as the Cu content increases, the $K\beta/K\alpha$ coefficient decreases. The results can play role in elemental material analysis, especially in archaeometry.

Keywords: FLUKA simulation; $K\beta/K\alpha$ intensity ratios; Ag-Cu alloy



Citation: Gójska, A.M.; Koziol, K.; Wasilewski, A.; Miśta-Jakubowska, E.A.; Mazerewicz, P.; Szymanowski, J. FLUKA Simulations of $K\beta/K\alpha$ Intensity Ratios of Copper in Ag–Cu Alloys. *Materials* **2021**, *14*, 4462. <https://doi.org/10.3390/ma14164462>

Received: 24 May 2021

Accepted: 7 August 2021

Published: 9 August 2021

Publisher's Note: MDPI stays neutral with regard to jurisdictional claims in published maps and institutional affiliations.



Copyright: © 2021 by the authors. Licensee MDPI, Basel, Switzerland. This article is an open access article distributed under the terms and conditions of the Creative Commons Attribution (CC BY) license (<https://creativecommons.org/licenses/by/4.0/>).

1. Introduction

The $K\beta/K\alpha$ intensity ratios have been intensively studied since 1969. Daoudi et al. [1] reports that after more than thousand measurements, 127 theoretical and experimental publications have been created in the last half century. The experimental measurements of X-ray spectra are crucial in examining theoretical models [2–4]. The values of $K\beta/K\alpha$ intensity ratios are used for estimation the vacancy transfer probability (e.g., transfer of hole from K shell to L shell [5–7]) and $K\alpha$ and $K\beta$ X-ray production cross-sections [8–11]. In experiments the excitation mediums were mainly radioisotopes: ^{241}Am [10,12–28], ^{109}Cd [29–31], ^{137}Cs [32,33], ^{57}Co [34], and ^{238}Pu [35]. X-ray tubes were also used for $K\beta/K\alpha$ intensity ratios studies [36–39] as well as proton beam [40,41].

There are a couple of aspects linked to the study on $K\beta/K\alpha$ intensity ratios. At first, experiments in which chemical compounds were tested showed that the $K\beta/K\alpha$ X-ray intensity ratios are sensitive to the chemical environment for $3d$ elements [13,20,42,43]. The results were explained by the change in screening of $3p$ electrons by $3d$ valence electrons. The studies on $3d$ metal alloys and compounds have shown dependence of the $K\beta/K\alpha$ intensity ratios on alloy composition or chemical state through changes in electron binding and electron configuration of the valence states [16]. Since Cu $3d$ states do not overlap energetically with the Ag $4d$ band, energy mismatch between Ag $4d$ and Cu $3d$ states is the main contributor to the sharpness and degeneracy of the Cu $3d$ states. Despite the lack of overlap of silver and copper wave functions in the Ag–Cu alloy, the charge density is transferred between Ag and Cu [44]. Raj et al. [17] report that in alloys the $3d$ electron transfer/delocalization is the main factor causing change in the $K\beta/K\alpha$ intensity ratios. Thus the changes in $K\beta/K\alpha$ intensity ratios of alloy's element indicate changes in the valence electronic configurations or charge transfer effect caused by presence of second elements [25]. The measurement of $K\beta/K\alpha$ intensity ratios can be a sensitive probe of $3d$ charge transfer [45].

Another advantage of $K\beta/K\alpha$ X-ray intensity ratio studies is that this parameter can be used for determination of depth profile distributions of the elements in thick targets [40].

This technique can be used in archaeometry to determine the silver enrichment taking place in antique silver–copper coins [39,46–48]. Since many decorative objects are composed of silvered copper, gilded copper, or silver, the use of $K\beta/K\alpha$ X-ray intensity ratio from different chemical element can allow estimating the thickness of the surface layer [49].

The knowledge on $K\beta/K\alpha$ X-ray intensity ratio can also be a tool to find elements which K or L lines overlap the lines of main element. So the $K\beta/K\alpha$ X-ray intensity ratio can be used to find the intensities of the unresolved lines of neighbor elements [50].

Research on $K\beta/K\alpha$ intensity ratios of complex materials motivated us the use of advanced Monte-Carlo tools, by means of the FLUKA code [51,52], to simulate complex X-ray spectra. The Monte-Carlo simulation method was introduced in 1949 and since then it has been successively used in many areas of physics, such as atomic physics, high energy physics, medical physics, as well as in material engineering, construction of accelerator structures, and in other fields of science, including mathematics, biology, economics, and archaeometry. Although the FLUKA code does not include in-depth quantum-mechanic features at atomic level such as the charge transfer between $3d$ electrons, in our paper the analytical challenge is based on a comprehensive and accurate description of the spectrum features such as the shape of the primary radiation spectrum, i.e., the intensity and the shape of the X-ray tube anode lines, and the intensity, the centroid, and the shape of all emission lines of the tested material. Each of the individual elements of the spectrum provides relevant analytical information. The simulation allows the determination of the $K\beta/K\alpha$ intensity ratios without the need to transform the radiation intensity of the characteristic sample obtained in the detector. Self-absorption and detector performance corrections, which are usually necessary in conventional quantitative analysis based on main peak analysis, are therefore eliminated, which means that the FLUKA code just simulates an experimental output, not a detector input. The reliability of Monte-Carlo tools, in addition to the subjective modeling of the composition and structure of the sample, depends on the analytical model adopted, the description of the radiation source, and the settings of equipment specifications, operational parameters, and experimental geometry. Since $K\beta/K\alpha$ intensity ratios of Cu have been extensively explored the simulation of this element is an appropriate test point.

In this work, X-ray spectra of silver–copper alloys were modeled. The copper $K\beta/K\alpha$ intensity ratios were calculated for pure Cu as well as for Ag–Cu alloys. Two kinds of the FLUKA simulations have been performed. The first kind includes primary electron beam and radiation of X-ray tube equipped with a Rh anode operating at 40.8 kV. The second kind includes a monoenergetic 59.9 keV photon beam. The fluorescence spectra of silver–copper alloys are an output for both kind of simulations. The results obtained are critically evaluated by comparison with available experimental and theoretical values for pure elements. It is worth underlining that the obtained results are not exactly the same kind as the experimental results. It is because the experimental results are based on the X-ray photons counted by the detector and then the values are corrected by detector efficiency and air and sample absorption coefficients. In contrast, the FLUKA simulation results are based on the X-ray photons emitted directly from the sample.

2. Experiment Simulations

Monte-Carlo simulations were performed using FLUKA 2011 code version 2c.8 installed on a computer cluster at Świerk Computing Center [53]. FLUKA code uses the Evaluated Photon Data Library (EPDL97) [54]. The EPDL library consists of tabulations of photon interaction data including photoionization, photoexcitation, coherent and incoherent scattering, and pair and triplet production cross sections.

The experimental setup reproduced in the calculations, consisting of an X-ray tube model with a 1 mm thick Rh anode, a 1 mm thick Be window, and two irradiated sample groups with a diameter of 1 cm and a thickness of 2 mm and 1 μm , is shown in Figure 1. Additionally, for samples with thickness of 1 μm the monoenergetic ^{241}Am (59.9 keV) have been used. As one can see from Figure 1, in the case of 1 μm sample a part of radiation

is going through the sample and another part is reflected back off the sample. The first part is called the forward output flux and the second part is called the backward output flux (this part is usually incoming to the detector). In the case of the 2 mm sample there is no forward output flux, because all radiation going through the sample is absorbed or re-emitted in a backward direction. Calculations for each alloy were made by dividing them into 500 parallel processes. The 1 keV photon and electron transport energy cut-off was set to best reproduce photon and electron behaviour for the used beam energy range. The Rh-X-ray was induced by a $2 \cdot 10^{11}$ monoenergetic electron beam (40.8 keV) with flat distribution, $\Phi = 1$ cm. The Rh anode X-ray spectrum filtered by a 1 mm Be layer is presented in Figure 2. The calculated K X-ray spectra of Ag–Cu alloy registered on a flat, irradiated sample surface are presented in Figure 3.

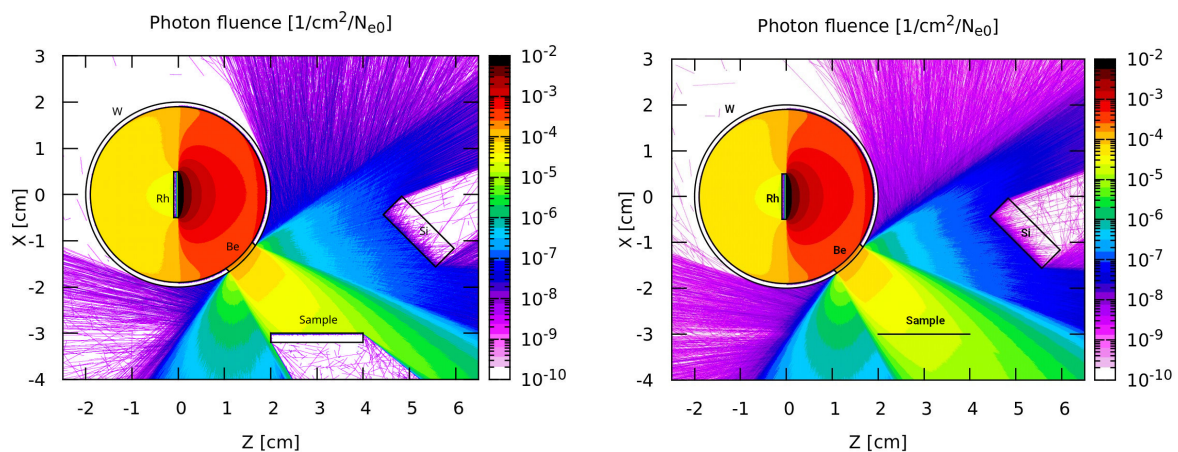


Figure 1. Experimental setup and photon fluence reproduced in the calculations for the sample thickness of 2 cm (left) and 1 μm (right).

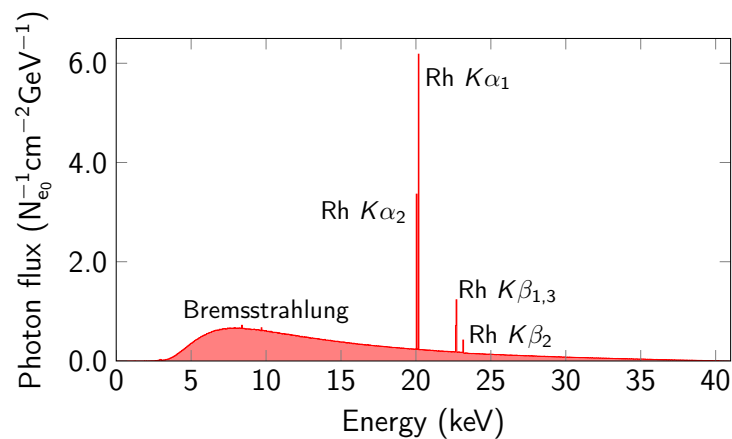


Figure 2. Rh anode X-ray spectrum.

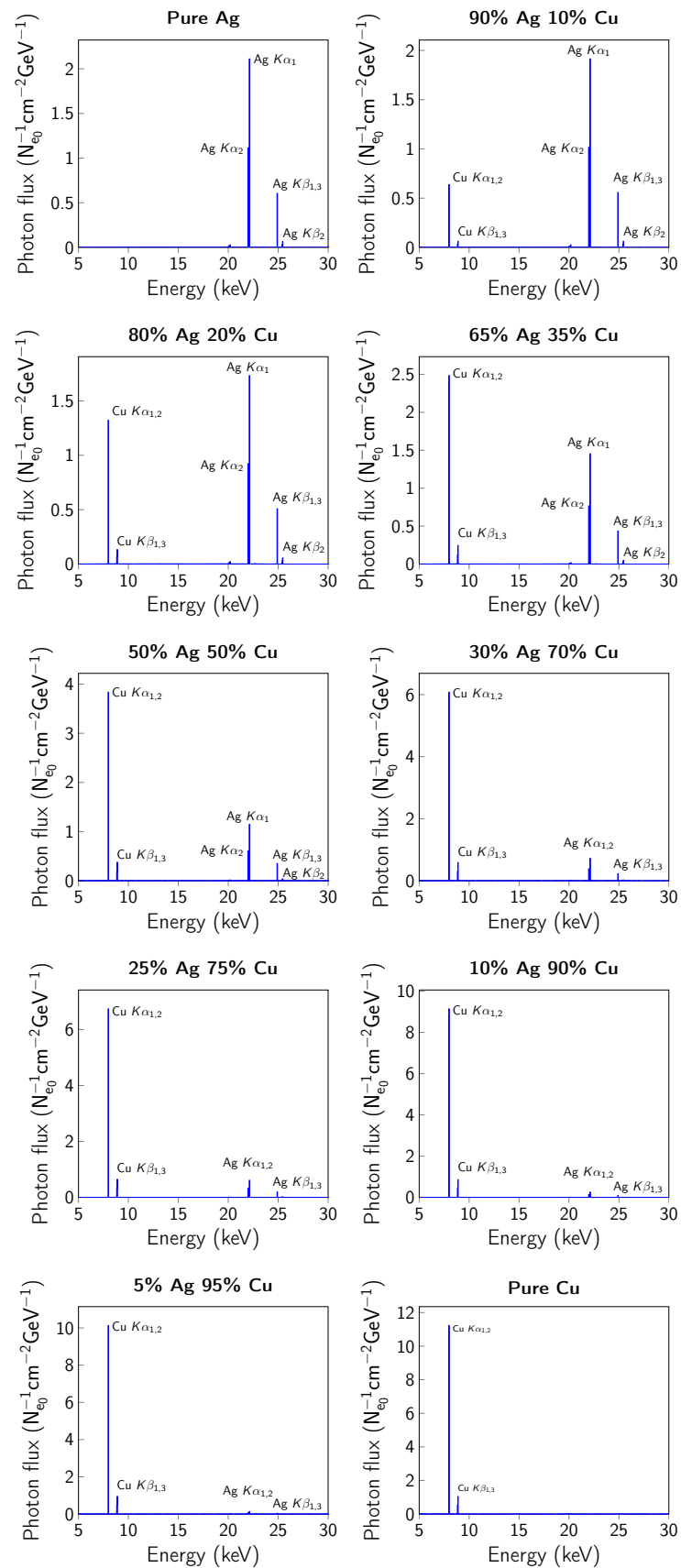


Figure 3. X-ray spectra in studied Ag–Cu alloys.

3. Results and Discussion

The simulated Cu $K\alpha$ and Cu $K\beta$ intensities as well as the different Ag–Cu alloys are presented in Tables 1–3. In our work we have considered the following K-x-ray transitions: $K\alpha_{1,2}$ ($K-L_{2,3}$), $K\beta_{1,3}$ ($K-M_{2,3}$), and $K\beta_2$ ($K-N_{2,3}$). The dependence of $K\beta/K\alpha$ intensity ratio on copper concentration in Ag–Cu alloy is presented in Figures 4–6. Three cases are studied: backward output flux, forward output flux, and weighted average output flux. The error bars arise from statistical uncertainties. In real experiment the errors are attributed to uncertainties from various parameters used in the determination of the $K\beta/K\alpha$ intensity ratio, including errors caused by the evaluation of peak area, detector efficiency, self-absorption factors, target thickness, and counting statistic. Table 4 presents the available theoretical and experimental values for pure copper while in Table 5 values for Cu alloys obtained from available literature. The literature data for pure Cu and Cu–Ag alloy are also presented collectively in Figures 4–6.

Some general conclusions can be drawn based on the presented data : (i) In the case of backward and average output fluxes, there is very small difference between results calculated for 1 μm sample for both Rh X-ray tube and monoenergetic 60 keV radiations, but here is distinct difference between these results and results calculated for the 2 mm sample. (ii) There is no forward output flux in the case of the 2 mm thick sample, because all radiation is absorbed in this direction while moving through the sample. For 1 μm samples the difference between results for Rh X-ray tube and monoenergetic radiations is bigger than in the case of backward output flux. (iii) As can be seen from Figure 4, a major part of experimental results is placed in between the FLUKA results calculated for very thin (1 μm) and very thick (2 mm) samples. The present results can also partially explain the differences between various experimental results for pure copper as a result of different thickness of samples used in experiments. (iv) The Cu $K\beta/K\alpha$ intensity ratio is sensitive to alloy composition. As the Cu content increases, the $K\beta/K\alpha$ coefficients decrease. The alloying effect is in order of a few percent and this size of effect is consistent with the size of the alloying effect reported by Dhal et al. [28].

Table 1. Simulated $K\beta/K\alpha$ intensity ratio for 1 μm thick samples induced by Rh X-ray tube radiation, calculated for backward and forward direction and weighted average of them.

Cu (%)	$K\beta/K\alpha$		
	Average	Backward Only	Forward Only
10	0.1285(12)	0.1283(12)	0.1373(81)
20	0.1292(8)	0.1289(8)	0.1367(41)
30	0.1286(7)	0.1282(7)	0.1358(28)
40	0.1285(6)	0.1281(6)	0.1335(21)
50	0.1282(5)	0.1277(5)	0.1336(17)
60	0.1278(5)	0.1272(5)	0.1328(14)
70	0.1275(4)	0.1269(4)	0.1320(13)
80	0.1272(4)	0.1265(4)	0.1318(11)
90	0.1266(4)	0.1259(4)	0.1308(10)
100	0.1269(4)	0.1263(5)	0.1299(10)

Table 2. Simulated $K\beta/K\alpha$ intensity ratio for 1 μm thick samples induced by monoenergetic radiation, calculated for backward and forward direction and weighted average of them.

Cu (%)	$K\beta/K\alpha$		
	Average	Backward Only	Forward Only
10	0.1299(2)	0.1300(3)	0.1298(3)
50	0.1277(1)	0.1275(1)	0.1280(1)
90	0.1258(1)	0.1258(1)	0.1258(1)
100	0.1253(1)	0.1254(1)	0.1253(1)

Table 3. Simulated $K\beta/K\alpha$ intensity ratio for 2 mm thick samples induced by Rh X-ray tube radiation. Only backward direction is calculated.

Cu (%)	$K\beta/K\alpha$
10	0.1474(19)
20	0.1498(13)
35	0.1470(9)
50	0.1462(7)
70	0.1447(6)
75	0.1433(6)
90	0.1406(5)
95	0.1402(4)
100	0.1392(4)

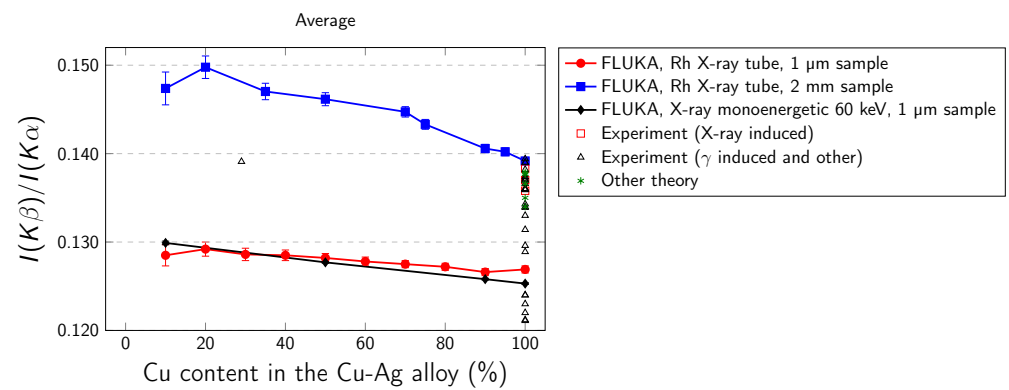


Figure 4. $K\beta/K\alpha$ intensity ratio arising from the primary X-ray simulated with FLUKA, calculated for average output flux in 1 μm and 2 cm samples.

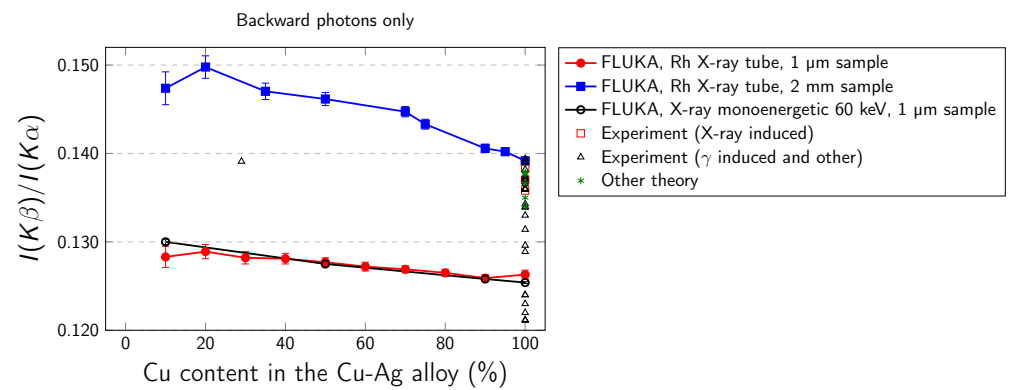


Figure 5. $K\beta/K\alpha$ intensity ratio arising from the primary X-ray simulated with FLUKA, calculated for backward output flux in 1 μm and 2 cm samples.

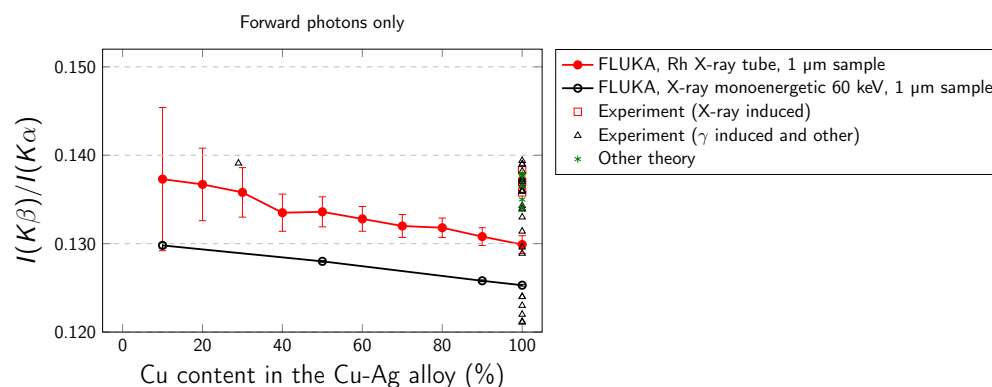


Figure 6. $K\beta/K\alpha$ intensity ratio arising from the primary X-ray simulated with FLUKA, calculated for forward output flux in 1 μm sample.

Table 4. $K\beta/K\alpha$ intensity ratio for copper taken from the literature.

$K\beta/K\alpha$	Reference	Excitation Source
Experiment:		
0.1382(16)	[12]	^{241}Am
0.1370(110)	[13]	^{241}Am
0.1330(33)	[14]	^{241}Am
0.1212(90)	[10]	^{241}Am
0.1211(19)	[15]	^{241}Am
0.1360(6)	[17]	^{241}Am
0.1340(130)	[18]	^{241}Am
0.1343(12)	[19]	^{241}Am
0.1374(113)	[20]	^{241}Am
0.1390(130)	[21]	^{241}Am
0.1220(100)	[22]	^{241}Am
0.1360(60)	[13]	^{241}Am
0.1359(30)	[24]	^{241}Am
0.1314(87)	[25]	^{241}Am
0.1289(86)	[26]	^{241}Am
0.1296(66)	[27]	^{241}Am
0.1360(10)	[28]	^{241}Am
0.1394(70)	[55]	^{241}Am
0.1360(60)	[35]	^{238}Pu
0.1366(330)	[56]	^{109}Cd
0.1370	[30]	^{109}Cd
0.1390(56)	[31]	^{109}Cd
0.1240(30)	[33]	^{137}Cs
0.1240(90)	[32]	^{137}Cs
0.1339	[34]	^{57}Co
0.1360(20)	[38]	K-capture
0.1372(10)	[41]	1 MeV protons
0.1358(17)	[36]	50 kV W X-ray tube
0.1383(55)	[37]	35 mA W X-ray tube
0.1370(20)	[38]	30 kV Mo X-ray tube
0.123(7)	[57]	10 keV synchrotron radiation
Theory:		
0.1379	[2]	
0.1377	[3]	
0.1340, 0.1350, 0.1366, 0.1377	[4] *	

* different approaches

Table 5. $K\beta/K\alpha$ intensity ratio and relative $K\beta/K\alpha$ ratio (compared to $K\beta/K\alpha$ ratio of pure Cu) for copper alloys taken from literature.

Cu Alloy	$K\beta/K\alpha$	Relative $K\beta/K\alpha$	Reference
Cu ₂₉ Ag ₇₁	0.1391(7)	-	[28]
Cu ₉₄ Sn ₆	0.1351(6)	-	[28]
Cu _{48.4} Sn _{51.6}	0.1419(72)	1.0949	[27]
Cu ₁₄ Sn ₈₆	0.1429(73)	1.1026	[27]
Cu _{6.1} Sn _{93.9}	0.1381(70)	1.0656	[27]
Co ₂₅ Cu ₇₄ Ag ₁	0.1388(92)	1.0563	[25]
Co ₃₁ Cu ₆₈ Ag ₁	0.1444(96)	1.0989	[25]
Co ₃₆ Cu _{63.6} Ag _{0.4}	0.1371(91)	1.0434	[25]
Co _{10.7} Cu _{89.1} Ag _{0.2}	0.1341(89)	1.0205	[25]
CuAl	0.1335(6)	-	[16]

4. Conclusions

The Cu $K\beta/K\alpha$ intensity ratios for pure copper and for a sequence of nine Ag–Cu alloys (from 10% to 100% Cu) have been simulated with the FLUKA code. The results can play role in elemental material analysis, especially in archaeometry. Silver and copper are used in jewelry and minting from antique times [39,58–60]. Thus it is in the interest of archaeologists to explore the ancient technologies of silver jewelry production. Copper was often added to silver to make sterling silver, increasing its strength. The concentration of more than 2.6% Cu indicates a deliberate addition by ancient manufacturers. The spectroscopic techniques like ED-XRF, SEM-EDX, or PIXE are commonly used in compositional research. The elemental content is determined by using intensity of peaks recorded in energetic spectra. However, these techniques can be used for surface and subsurface analysis. The $K\beta/K\alpha$ X-ray intensity ratio analyses can be applied for elemental composition analysis as well as for determination of depth profile distributions of the elements in studied artifacts. The thickness of coating in double layers artifacts and silver surface enrichment of silver–copper alloys can be also determined. Moreover, since the Ag–Cu alloying system has many other applications, among others it is often used in nanotechnology [61,62] and it is estimated as the best material for improving oxidation resistance with only a slight reduction in electrical conductivity [63], knowledge about alloying effects may play important role in those areas.

Author Contributions: A.M.G.: conceptualization, methodology, writing—original draft. K.K.: investigation, formal analysis, writing—review and editing, visualization. A.W.: investigation, formal analysis, writing—review and editing, visualization. E.A.M.-J.: investigation, writing—review and editing. P.M.: investigation, writing—review and editing. J.S.: investigation, writing—review and editing. All authors have read and agreed to the published version of the manuscript.

Funding: This research received no external funding.

Institutional Review Board Statement: Not applicable.

Informed Consent Statement: Not applicable.

Data Availability Statement: The data presented in this study are available on request from the corresponding author.

Acknowledgments: The authors are grateful to Jacek Ratajczyk for providing language help.

Conflicts of Interest: The authors declare no conflict of interest.

References

- Daoudi, S.; Kahoul, A.; Kup Aylikci, N.; Sampaio, J.; Marques, J.; Aylikci, V.; Sahnoune, Y.; Kasri, Y.; Deghfel, B. Review of experimental photon-induced $K\beta/K\alpha$ intensity ratios. *At. Data Nucl. Data Tables* **2020**, *132*, 101308. [[CrossRef](#)]
- Scofield, J.H. Exchange corrections of K x-ray emission rates. *Phys. Rev. A* **1974**, *9*, 1041–1049. [[CrossRef](#)]
- Jankowski, K.; Polasik, M. On the calculation of $K\beta/K\alpha$ X-ray intensity ratios. *J. Phys. At. Mol. Opt. Phys.* **1989**, *22*, 2369–2376. [[CrossRef](#)]

4. Polasik, M. Influence of changes in the valence electronic configuration on the $K\beta$ -to- $K\alpha$ X-ray intensity ratios of the 3d transition metals. *Phys. Rev. A* **1998**, *58*, 1840–1845. [[CrossRef](#)]
5. Ertugral, B.; Cevik, U.; Tirasoglu, E.; Kopya, A.; Ertugrul, M.; Dogan, O. Measurement of K to L shell vacancy transfer probabilities for the elements $52 \leq Z \leq 68$. *J. Quant. Spectrosc. Radiat. Transf.* **2003**, *78*, 163–169. [[CrossRef](#)]
6. Ertugral, B.; Baltas, H.; Celik, A.; Kobyay, Y. Vacancy Transfer Probabilities from K to L Shell for Low Atomic Number Elements at 5.96 keV. *Acta Phys. Pol. A* **2010**, *117*, 900–903. [[CrossRef](#)]
7. Puri, S.; Mehta, D.; Chand, B.; Singh, N.; Trehan, P. Measurements of K to L shell vacancy transfer probability for the elements $37 \leq Z \leq 42$. *Nucl. Instrum. Methods Phys. Res. Sect. B Beam Interact. Mater. Atoms* **1993**, *73*, 443–446. [[CrossRef](#)]
8. Durak, R.; Özdemir, Y. Measurement of K-shell fluorescence cross-sections and yields of 14 elements in the atomic number range $25 \leq Z \leq 47$ using photoionization. *Radiat. Phys. Chem.* **2001**, *61*, 19–25. [[CrossRef](#)]
9. Şahin, M.; Demir, L.; Budak, G. Measurement of K X-ray fluorescence cross-sections and yields for 5.96 keV photons. *Appl. Radiat. Isot.* **2005**, *63*, 141–145. [[CrossRef](#)] [[PubMed](#)]
10. Yılmaz, R. $K\beta/K\alpha$ X-ray intensity ratios for some elements in the atomic number range $28 \leq Z \leq 39$ at 16.896 keV. *J. Radiat. Res. Appl. Sci.* **2017**, *10*, 172–177. [[CrossRef](#)]
11. Küçükönder, A.; Söğüt, Ö.; Büyükkasap, E.; Küçükönder, E.; Çam, H. $K\beta/K\alpha$ x-ray intensity ratios for bromine and iodine compounds. *X-ray Spectrom.* **2003**, *32*, 60–63. [[CrossRef](#)]
12. Casnati, E.; Tartari, A.; Baraldi, C.; Napoli, G. Measurement of the $K\beta/K\alpha$ yield ratios of Cu, Mo and Cd stimulated by 59.54 keV photons. *J. Phys. B At. Mol. Phys.* **1985**, *18*, 2843–2849. [[CrossRef](#)]
13. Çevik, U.; Değirmencioglu, İ.; Ertugral, B.; Apaydin, G.; Baltas, H. Chemical effects on the $K\beta/K\alpha$ X-ray intensity ratios of Mn, Ni and Cu complexes. *Eur. Phys. J. D* **2005**, *36*, 29–32. [[CrossRef](#)]
14. Coelho, L.F.S.; Gaspar, M.B.; Eichler, J. $K\beta$ -to- $K\alpha$ x-ray intensity ratios after ionization by γ rays. *Phys. Rev. A* **1989**, *40*, 4093–4096. [[CrossRef](#)]
15. Küçükönder, A.; Şahin, Y.; Büyükkasap, E. Dependence of the $K\beta/K\alpha$ intensity ratio on the oxidation state. *J. Radioanal. Nucl. Chem. Artic.* **1993**, *170*, 125–132. [[CrossRef](#)]
16. Padhi, H.C.; Dhal, B. X-ray intensity ratios of Fe, Co, Ni, Cu, Mo, Ru, Rh and Pd in equiatomic aluminides. *Solid State Commun.* **1995**, *96*, 171–173. [[CrossRef](#)]
17. Raj, S.; Dhal, B.B.; Padhi, H.C.; Polasik, M. Influence of solid-state effects on the $K\beta$ -to- $K\alpha$ x-ray intensity ratios of Ni and Cu in various silicide compounds. *Phys. Rev. B* **1998**, *58*, 9025–9029. [[CrossRef](#)]
18. Ertugrul, M.; Söğüt, Ö.; Şimşek, Ö.; Büyükkasap, E. Measurement of $K\beta/K\alpha$ intensity ratios for elements in the range $22 \leq Z \leq 69$ at 59.5 keV. *J. Phys. B At. Mol. Opt. Phys.* **2001**, *34*, 909–914. [[CrossRef](#)]
19. Raj, S.; Padhi, H.C.; Palit, P.; Basa, D.K.; Polasik, M.; Pawłowski, F. Relative K x-ray intensity studies of the valence electronic structure of 3d transition metals. *Phys. Rev. B* **2002**, *65*, 193105. [[CrossRef](#)]
20. Söğüt, Ö.; Baydaş, E.; Büyükkasap, E.; Şahin, Y.; Küçükönder, A. Chemical effects on L shell fluorescence yields of Ba, La and Ce compounds. *J. Radioanal. Nucl. Chem.* **2002**, *251*, 119–122. [[CrossRef](#)]
21. Öz, E. Determination of ratios of emission probabilities of Auger electrons and K–L-shell radiative vacancy transfer probabilities for 17 elements from Mn to Mo at 59.5 keV. *J. Quant. Spectrosc. Radiat. Transf.* **2006**, *97*, 41–50. [[CrossRef](#)]
22. Han, I.; Şahin, M.; Demir, L.; Şahin, Y. Measurement of K X-ray fluorescence cross-sections, fluorescence yields and intensity ratios for some elements in the atomic range $22 \leq Z \leq 68$. *Appl. Radiat. Isot.* **2007**, *65*, 669–675. [[CrossRef](#)]
23. Cevik, U.; Kaya, S.; Ertugral, B.; Baltas, H.; Karabıdak, S. K-shell X-ray fluorescence cross-sections and intensity ratios for some pure metals at 59.5 and 123.6 keV. *Nucl. Instrum. Methods Phys. Res. Sect. B Beam Interact. Mater. Atoms* **2007**, *262*, 165–170. [[CrossRef](#)]
24. Ertugral, B.; Apaydin, G.; Çevik, U.; Ertugrul, M.; Kobyay, A.I. $K\beta/K\alpha$ X-ray intensity ratios for elements in the range $16 \leq Z \leq 92$ excited by 5.9, 59.5 and 123.6 keV photons. *Radiat. Phys. Chem.* **2007**, *76*, 15–22. [[CrossRef](#)]
25. Aylikci, N.K.; Tıraşođlu, E.; Apaydin, G.; Cengiz, E.; Aylikci, V.; Bakkalođlu, Ö.F. Influence of alloying effect on X-ray fluorescence parameters of Co and Cu in CoCuAg alloy films. *Chem. Phys. Lett.* **2009**, *475*, 135–140. [[CrossRef](#)]
26. Akkuş, T.; Şahin, Y.; Yılmaz, D.; Tuzluca, F.N. The K-beta/K-alpha intensity ratios of some elements at different azimuthal scattering angles at 59.54 keV. *Can. J. Phys.* **2017**, *95*, 220–224. [[CrossRef](#)]
27. Dogan, M.; Olgar, M.; Cengiz, E.; Tıraşođlu, E. Alloying effect on K shell X-ray fluorescence cross-sections and intensity ratios of Cu and Sn in Cu 1 Sn 1-x alloys using the 59.5 keV gamma rays. *Radiat. Phys. Chem.* **2016**, *126*, 111–115. [[CrossRef](#)]
28. Dhal, B.B.; Padhi, H.C. Relative K x-ray intensities in some selected elements between Mn and Sb following ionization by 59.54-keV γ rays. *Phys. Rev. A* **1994**, *50*, 1096–1100. [[CrossRef](#)] [[PubMed](#)]
29. Porikli, S.; Demir, D.; Kurucu, Y. Chemical Effects on X-ray Emission Spectrum of Some Mn and Fe Compounds. *Balk. Phys. Lett.* **2008**, 431–436.
30. Kaçal, M.R.; Han, İ.; Akman, F. Determination of K shell absorption jump factors and jump ratios of 3d transition metals by measuring K shell fluorescence parameters. *Appl. Radiat. Isot.* **2015**, *95*, 193–199. [[CrossRef](#)]
31. Han, I.; Demir, L. Effect of annealing treatment on $K\beta$ -to- $K\alpha$ x-ray intensity ratios of 3D transition-metal alloys. *Phys. Rev. A* **2010**, *81*, 062514. [[CrossRef](#)]
32. Anand, L.F.M.; Gudennavar, S.B.; Bubbly, S.G.; Kerur, B.R. K β to K α X-ray intensity ratios and K to L shell vacancy transfer probabilities of Co, Ni, Cu, and Zn. *J. Exp. Theor. Phys.* **2015**, *121*, 961–965. [[CrossRef](#)]

33. Anand, L.F.M.; Gudennavar, S.B.; Bubbly, S.G.; Kerur, B.R. K-Shell X-ray Fluorescence Parameters of a Few Low Z Elements. *J. Exp. Theor. Phys.* **2018**, *126*, 1–7. [CrossRef]
34. Hansen, J.; Freund, H.; Fink, R. Relative X-ray transition probabilities to the K-shell. *Nucl. Phys. A* **1970**, *142*, 604–608. [CrossRef]
35. Venkateswara Rao, N.; Bhuloka Reddy, S.; Satyanarayana, G.; Sastry, D. $K\beta/K\alpha$ X-ray intensity ratios in elements with $20 \leq Z \leq 50$. *Physica B+C* **1986**, *138*, 215–218. [CrossRef]
36. Bé, M.M.; Lépy, M.C.; Plagnard, J.; Duchemin, B. Measurement of relative X-ray intensity ratios for elements in the $22 \leq Z \leq 29$ Region. *Appl. Radiat. Isot.* **1998**, *49*, 1367–1372. [CrossRef]
37. McCrary, J.H.; Singman, L.V.; Ziegler, L.H.; Looney, L.D.; Edmonds, C.M.; Harris, C.E. K-Fluorescent-X-ray Relative-Intensity Measurements. *Phys. Rev. A* **1971**, *4*, 1745–1750. [CrossRef]
38. Paić, G.; Pečar, V. Study of anomalies in $K\beta/K\alpha$ ratios observed following K-electron capture. *Phys. Rev. A* **1976**, *14*, 2190–2192. [CrossRef]
39. Gójska, A.M.; Koziół, K.; Mišta-Jakubowska, E.A.; Diduszko, R. Determination of the $K\beta/K\alpha$ intensity ratios of silver in Ag-Cu alloys. *Nucl. Instrum. Methods Phys. Res. Sect. B Beam Interact. Mater. Atoms* **2020**, *468*, 65–70. [CrossRef]
40. Ahlberg, M. Simple depth profile determination by proton-induced x-ray emission. *Nucl. Instrum. Methods* **1975**, *131*, 381–384. [CrossRef]
41. Perujo, A.; Maxwell, J.A.; Teesdale, W.J.; Campbell, J.L. Deviation of the $K\beta/K\alpha$ intensity ratio from theory observed in proton-induced X-ray spectra in the $22 \leq Z \leq 32$ region. *J. Phys. B At. Mol. Phys.* **1987**, *20*, 4973–4982. [CrossRef]
42. Brunner, G.; Nagel, M.; Hartmann, E.; Arndt, E. Chemical sensitivity of the $K\beta/K\alpha$ X-ray intensity ratio for 3d elements. *J. Phys. At. Mol. Phys.* **1982**, *15*, 4517–4522. [CrossRef]
43. Mukoyama, T.; Taniguchi, K.; Adachi, H. Variation of $K\beta/K\alpha$ x-ray intensity ratios in 3d elements. *X-ray Spectrom.* **2000**, *29*, 426–429. [CrossRef]
44. Greiner, M.T.; Jones, T.E.; Beeg, S.; Zwiener, L.; Scherzer, M.; Girgsdies, F.; Piccinin, S.; Armbrüster, M.; Knop-Gericke, A.; Schlögl, R. Free-atom-like d states in single-atom alloy catalysts. *Nat. Chem.* **2018**, *10*, 1008–1015. [CrossRef]
45. Bhuinya, C.R.; Padhi, H.C. Alloying effect on the K beta /K alpha intensity ratios of Ti, Cr and Ni. *J. Phys. B At. Mol. Opt. Phys.* **1992**, *25*, 5283–5287. [CrossRef]
46. Linke, R.; Schreiner, M. Energy Dispersive X-Ray Fluorescence Analysis and X-Ray Microanalysis of Medieval Silver Coins. *Microchim. Acta* **2000**, *133*, 165–170. [CrossRef]
47. Linke, R.; Schreiner, M.; Demortier, G. The application of photon, electron and proton induced X-ray analysis for the identification and characterisation of medieval silver coins. *Nucl. Instrum. Methods Phys. Res. Sect. B Beam Interact. Mater. Atoms* **2004**, *226*, 172–178. [CrossRef]
48. Beck, L.; Bosonnet, S.; Réveillon, S.; Eliot, D.; Pilon, F. Silver surface enrichment of silver–copper alloys: A limitation for the analysis of ancient silver coins by surface techniques. *Nucl. Instrum. Methods Phys. Res. Sect. B Beam Interact. Mater. Atoms* **2004**, *226*, 153–162. [CrossRef]
49. Cesareo, R.; de Assis, J.T.; Roldán, C.; Bustamante, A.D.; Brunetti, A.; Schiavon, N. Multilayered samples reconstructed by measuring $K\alpha/K\beta$ or $L\alpha/L\beta$ X-ray intensity ratios by EDXRF. *Nucl. Instrum. Methods Phys. Res. Sect. B Beam Interact. Mater. Atoms* **2013**, *312*, 15–22. [CrossRef]
50. Khan, M.R.; Karimi, M. $K\beta/K\alpha$ ratios in energy-dispersive x-ray emission analysis. *X-ray Spectrom.* **1980**, *9*, 32–35. [CrossRef]
51. Böhlen, T.; Cerutti, F.; Chin, M.; Fassò, A.; Ferrari, A.; Ortega, P.; Mairani, A.; Sala, P.; Smirnov, G.; Vlachoudis, V. The FLUKA Code: Developments and Challenges for High Energy and Medical Applications. *Nucl. Data Sheets* **2014**, *120*, 211–214. [CrossRef]
52. Ferrari, A.; Sala, P.; Fassò, A.; Ranft, J. *FLUKA: A Multi-Particle Transport Code*; Technical Report October; Stanford Linear Accelerator Center (SLAC): Menlo Park, CA, USA, 2005. [CrossRef]
53. Świerk Computing Centre. Infrastructure and Services for Power Industry. Available online: <http://www.cis.gov.pl/> (accessed on 9 August 2021).
54. Cullen, D.; Hubbell, J.; Kissel, L. *EPDL97: The Evaluated Photo Data Library '97 Version*; Technical report; Lawrence Livermore National Laboratory (LLNL): Livermore, CA, USA, 1997. [CrossRef]
55. Uğurlu, M.; Demir, L. Relative K X-ray intensity ratios of the first and second transition elements in the magnetic field. *J. Mol. Struct.* **2020**, *1203*, 127458. [CrossRef]
56. Porikli, S.; Kurucu, Y. Effect of an External Magnetic Field on the $K\alpha$ and $K\beta$ x-Ray Emission Lines of the 3d Transition Metals. *Instrum. Sci. Technol.* **2008**, *36*, 341–354. [CrossRef]
57. Mirji, S.; Bennal, A.; Krishnananda; Badiger, N.; Tiwari, M.; Lodha, G. Determination of K-L vacancy transfer probabilities of some 3d elements using synchrotron radiation. *Can. J. Phys.* **2015**, *93*, 760–764. [CrossRef]
58. Mišta-Jakubowska, E.A.; Fijał-Kirejczyk, I.; Diduszko, R.; Gójska, A.M.; Kalbarczyk, P.; Milczarek, J.J.; Trela, K.; Żabiński, G. A silvered shield grip from the Roman Period: a technological study of its silver coating. *Archaeol. Anthropol. Sci.* **2019**, *11*, 3343–3355. [CrossRef]
59. Mišta-Jakubowska, E.; Czech Błońska, R.; Duczko, W.; Gójska, A.M.; Kalbarczyk, P.; Żabiński, G.; Trela, K. Archaeometric studies on early medieval silver jewellery from Central and Eastern Europe. *Archaeol. Anthropol. Sci.* **2019**, *11*, 6705–6723. [CrossRef]
60. Gójska, A.; Mišta-Jakubowska, E.; Banaś, D.; Kubala-Kukuś, A.; Stabrawa, I. Archaeological applications of spectroscopic measurements. Compatibility of analytical methods in comparative measurements of historical Polish coins. *Measurement* **2019**, *135*, 869–874. [CrossRef]

-
61. Abdul Salam, A.; Singaravelan, R.; Vasanthi, P.; Bangarusudarsan Alwar, S. Electrochemical fabrication of Ag–Cu nano alloy and its characterization: An investigation. *J. Nanostruct. Chem.* **2015**, *5*, 383–392. [[CrossRef](#)]
 62. Paszkiewicz, M.; Gołębiewska, A.; Rajski, Ł.; Kowal, E.; Sajdak, A.; Zaleska-Medynska, A. The Antibacterial and Antifungal Textile Properties Functionalized by Bimetallic Nanoparticles of Ag/Cu with Different Structures. *J. Nanomater.* **2016**, *2016*, 6056980. [[CrossRef](#)]
 63. Kim, K.O.; Kim, S. Surface Morphology Control of Cu–Ag Alloy Thin Film on W Diffusion Barrier by Seedless Electrodeposition. *J. Nanosci. Nanotechnol.* **2016**, *16*, 11701–11706. [[CrossRef](#)]